# Carbon-Based Nanostructures Obtained in Water by Ultrashort Laser Pulses

**ARTICLE** *in* THE JOURNAL OF PHYSICAL CHEMISTRY C · MARCH 2011

Impact Factor: 4.77 · DOI: 10.1021/jp1094239



**10 AUTHORS**, INCLUDING:

A. Santagata
Italian National Research Council
**99** PUBLICATIONS **1,047** CITATIONS
SEE PROFILE

Alessandro De Giacomo
Università degli Studi di Bari Aldo Moro
**78** PUBLICATIONS **1,717** CITATIONS
SEE PROFILE

Alessandro Laurita
Università degli Studi della Basilicata
**18** PUBLICATIONS **194** CITATIONS
SEE PROFILE

Roberto Teghil
Università degli Studi della Basilicata
**161** PUBLICATIONS **1,779** CITATIONS
SEE PROFILE

THE JOURNAL OF PHYSICAL CHEMISTRY C

ARTICLE

pubs.acs.org/JPCC

# Carbon-Based Nanostructures Obtained in Water by Ultrashort Laser Pulses

A. Santagata,[†] A. De Bonis,[*,†,‡] A. De Giacomo,[§,⊥] M. Dell'Aglio,[⊥] A. Laurita,[‡] G. S. Senesi,[⊥] R. Gaudiuso,[§] S. Orlando,[†] R. Teghil,[†,‡] and G. P. Parisi[†]

[†]IMIP-CNR, U.O.S. Potenza, Via S. Loja, Zona Ind., 85050 Tito Scalo (PZ), Italy

[‡]Department of Chemistry "A.M. Tamburro", University of Basilicata, Via dell'Ateneo Lucano 10, 85100 Potenza, Italy

[§]Department of Chemistry, University of Bari "A. Moro", via Orabona 4, 70126, Bari, Italy

[⊥]IMIP-CNR, U.O.S. Bari, via Amendola 122/D, 70126, Bari, Italy

**ABSTRACT:** An ultrashort (100 fs) Ti:Sapphire pulsed laser has been employed in order to produce nanostructures by pulsed ablation of a graphite target in water. Different (10−100−1000 Hz) repetition rates have been used, and the features of material produced have been investigated by surface enhanced Raman spectroscopy (SERS) and scanning electron microscopy (SEM). SERS spectra show that a broad asymmetric band associated with diamond-like carbon (DLC) is observed when repetition rates of 10 or 100 Hz are used. On the contrary, ablated species produced with 1 kHz pulses present a narrow peak at 1333 $cm^{-1}$, the typical mode of diamond, which is, however, embedded in a DLC band centered at 1540 $cm^{-1}$. SEM images show the presence of dispersed octahedral-shaped structures having a size from 1 to 5 $\mu$m, in the case of 10 or 100 Hz repetition rates, and agglomerates of particles having a dimension below 300 nm, when 1 kHz pulses are used.

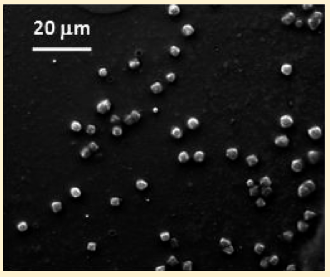


## 1. INTRODUCTION

In the last two decades, pulsed laser ablation (PLA) has been widely demonstrated to be a suitable method for diverse technological applications, such as deposition of thin films, micromachining, material surface treatment and cleaning, analytic diagnostics (laser-induced breakdown spectroscopy, laser ablation inductively coupled plasma mass spectrometry), and various nanoparticle (NP) production. The use of different laser parameters (wavelength, pulse intensity, repetition rate, and pulse duration) may strongly affect the laser−matter interaction processes and consequently the potential of laser ablation employment. With this regard, ultrashort (femtosecond−picosecond) laser pulses have opened new opportunities to be still exploited about the further uses of laser ablation for technological and research purposes. For instance, femtosecond laser pulses have the peculiarity of avoiding thermal effects induced in materials by nanosecond or longer pulses. It has been demonstrated that, during the use of ultrashort laser pulses, the ablated species can be characterized by properties very different from those due to nanosecond pulses. On the basis of plasma features observed in vacuum, it has been pointed out that the femtosecond pulses generate two components, the first formed by highly excited species, and the second, which is 2 orders of magnitude slower than the former, made of nanoparticles retaining, in several circumstances, the starting target composition.

The ultrashort PLA mechanism is still a matter of debate; nevertheless, it is widely accepted that a femtosecond laser pulse duration is shorter than the full ablation process. This involves, first, the excitation of material thin layer electrons by laser photon absorption, then material lattice relaxation by electron−phonon coupling, and finally the plasma formation. Thus, unlike the nanosecond pulse induced process, the ablated species formed by pulse femtosecond lasers do not interact with the laser pulse itself. Despite the lack of laser plasma interaction during ultrashort PLA performed in vacuum, it has been observed that the excited species can expand 1 order of magnitude faster than those obtained by nanosecond laser pulses.

In comparison to these pulse durations, the femtosecond PLA displays different features, such as species excitation temperatures, densities, and species dynamics, whose peculiarities can be key factors for setting off new opportunities for PLA in technological applications and material synthesis. When PLA is performed in a gas environment, the induced plasma undergoes to fast quenching and spatial confinement, which, once more, differ when a femtosecond or a nanosecond laser pulse is used. The experimental differences occurring when PLAs are performed by nanosecond or femtosecond pulses, in both vacuum or gas environments, suggest that, even when a PLA process is carried out in a liquid, the use of femtosecond laser pulses might offer different results than the ones obtainable by longer pulse durations. With this regard, Ogale et al.[1] have shown that nanostructured diamond materials can be well synthesized by PLAs in liquid environments.[2−11] Different from in vacuum experiments, the presence of a confining liquid can greatly affect

**Special Issue:** Laser Ablation and Nanoparticle Generation in Liquids

**Received:** October 1, 2010
**Revised:** January 27, 2011
**Published:** February 20, 2011





dx.doi.org/10.1021/jp1094239 | J. Phys. Chem. C 2011, 115, 5160–5164

the thermodynamics and kinetic evolution properties of PLA-induced plasmas, and it can play a significant role for the ablated species condensation process, which could promote the formation, even as metastable phases, of nanostructured materials. As shown by Yang et al. in their work published in 1998[12] and following,[3,8,11,13−15] $P$ and $T$ values of 10−15 GPa and 4000−5000 K, respectively, promote the phase transition of graphitic carbon into nanodiamonds (NDs). The size of the NDs' nuclei formed in a liquid environment has been related to thermodynamic parameters as well as the laser pulse duration.[7,8,10,13−15]

With regard to femtosecond PLA in liquid, the $T$ and $P$ can be 2−4 fold higher than those due to nanosecond laser sources[16] so that NDs larger than tens of nanometers in diameter[10] could be expected. Therefore, new opportunities for ND synthesis can be offered by PLA performed in liquid when an ultrashort laser pulse width is employed. With this purpose, the following work has been carried out considering a 100 fs laser pulse and the graphite−water system. Taking into account the results of studies published on PLA of this solid−liquid system, we have focused our attention on ND production changes caused by a simple laser pulse parameter variation, that is, the repetition rate (1−100−1000 Hz). For investigating the features of the material produced, surface enhanced Raman spectroscopy (SERS) and scanning electron microscopy (SEM) have been employed.

## 2. EXPERIMENTAL METHODS

In this work, an ultrashort Ti:Sapphire pulsed laser source (Spectra Physics Spitfire Pro XP, 800 nm, 2.7 mJ, 100 fs) having changeable repetition rates (1−1000 Hz) was used. The laser beam was focused perpendicularly to the target graphite plane surface by a 5 cm plano-convex focal length lens. The graphite solid samples covered by a 2 cm water column were contained in a standard spectroscopic UV quartz cuvette (3.5 mL). A micrometer translation stage was employed in order to minimize deep crater formation on the solid sample surface due to successive laser beam pulses.

Three different laser ablation repetition rates were used (10 Hz, 100 Hz, and 1 kHz). To compare the results obtained by these different repetition rates, the same number of laser pulses were considered: 2, 20, and 200 min for 1 kHz, 100 Hz, and 10 Hz, respectively. In any case, all ablation processes were performed in milli-Q water previously enriched with Ag NPs (diameter of about 10−20 nm[17−19]) obtained by 5 min of femtosecond pulsed ablation of a Goodfellow Ag foil (99.95% purity, 6 mm thickness). The Ag colloidal water solutions were controlled in order to be always comparable to each other by using their absorbance spectrum (Figure 1) obtained by diverting along another experimental branch 0.1% of the energy of the main femtosecond laser beam. This portion of the laser beam was focused on a 2 mm sapphire plate by a 10 cm plano-convex focal length lens producing a broad light continuum spectrum (300−500 nm) by multiphoton nonlinear effects. The Ag colloidal water solutions' absorbance was evaluated by removing the contribution of the cuvette containing milli-Q water. The transmitted light was dispersed, acquired, and processed by the use of an ARC 300i monocromator (1200 g/mm grating) linked to a PIXIS Princeton CCD detector and WinSpec 32 software.

The Ag NP solutions were used for detecting by SERS the material species produced by ultrashort PLA of graphite in water. In this way, an adequate amplification can be achieved of the Raman-active modes, which are nonresonant with a HeNe laser

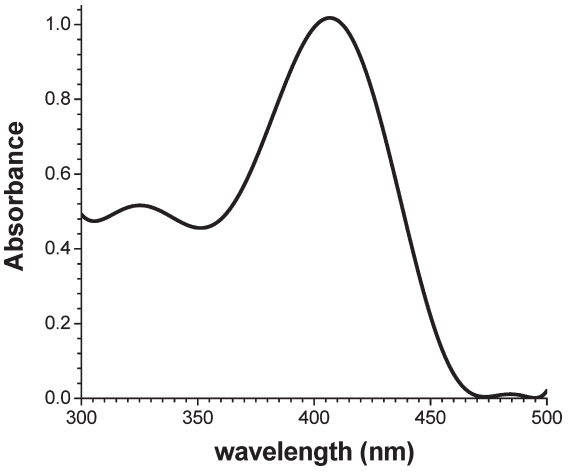


**Figure 1.** Typical vis absorbance spectrum of Ag nanoparticle colloidal water solutions used.

source. The Ag NPs together with the ultrashort PLA produced species were collected from the water solution by a pipet and deposited drop by drop on a Si(111) substrate. A total of three solution drops were used, adding the following drop only when the previous one was completely dried after its exposure to room temperature and atmospheric pressure. In this way, a good dispersion of the PLA species induced could be obtained so that SEM images and SERS spectra of isolated structures could be measured. These spectra were acquired by a micro-Raman Jobin Yvon (LABRAM HR800) in backscattered configuration equipped with two gratings (600 and 1800 g/mm) and an optical Olympus microscope having 10×, 50×, and 100× objectives. The spectrometer was connected to a liquid-$N_2$-cooled CCD detector. The excitation was obtained by using a HeNe laser source ($\lambda$ = 632.8 nm). The laser power was maintained at 20 mW, whereas the spectra were acquired using the 600 g/mm grating and the 100× objective. In this condition, the estimated spectrum resolution was about 4 $cm^{-1}$. The SEM images were obtained by a Philips-Fei ESEM XL30-$LaB_6$ after coating each sample by sputtering with a thin Au layer (ca. 10 nm).

## 3. RESULTS AND DISCUSSION

SERS spectra (Figures 2−4) show that a change of the laser beam repetition rate determines the deposition of different species. When laser frequencies of 10 or 100 Hz are used, a broad asymmetric band is observed within the Raman shift range of 1000−1725 $cm^{-1}$, which is associated with diamond-like carbon (DLC). Raman spectra of DLC species are known to show the characteristic so-called D (∼1360 $cm^{-1}$) and G (∼1560 $cm^{-1}$) peaks. The G band, which is related to $E_{2g}$ symmetry for graphite, is caused by the in-plane bond-stretching motion of a couple of $sp^2$ carbons, whereas the D feature, which is due to a breathing mode of $A_{1g}$ symmetry, is activated by the presence of $sp^2$ disordered structures.[20,21] Figures 2 and 3, which are obtained at laser ablation rates of 10 and 100 Hz, show the presence of additional Raman bands centered at 1970, 2125, and 3490 $cm^{-1}$, which can be assigned to CC stretchings of a mixture of different lengths of cumulene and polyyne chains[22−27] and of O−H stretchings, respectively. On the contrary, Figure 4, which refers to ablated species obtained at a laser frequency rate of 1 kHz, shows a narrow peak at 1333 $cm^{-1}$ assigned to the typical vibrational mode of diamond that is, however, embedded into the


dx.doi.org/10.1021/jp1094239 |J. Phys. Chem. C 2011, 115, 5160–5164

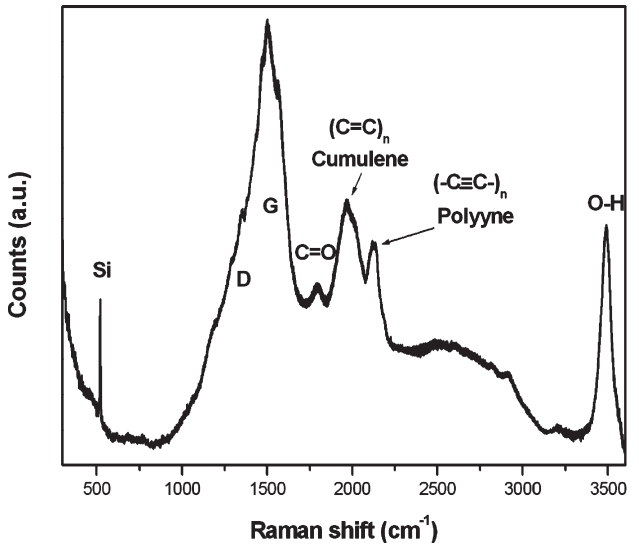


**Figure 2.** SERS spectrum of dried drops of Ag NP colloidal water solution mixed together with PLA species produced by a laser repetition frequency of 10 Hz. Si(111) substrate.

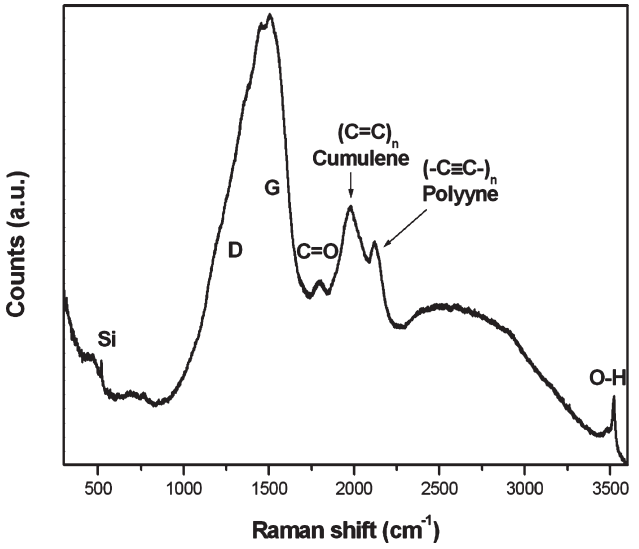


**Figure 3.** SERS spectrum of dried drops of Ag NP colloidal water solution mixed together with PLA species produced by a laser repetition frequency of 100 Hz. Si(111) substrate.

DLC band centered at 1540 $cm^{-1}$. However, the bands at 1580 and 1350 $cm^{-1}$, respectively, typical of crystalline or microcrystalline graphite phonons, are not present.

Using a 1 kHz laser repetition rate, the presence of bands centered at 1805 and 2830−2930 $cm^{-1}$ is observed. The narrow band at 1805 $cm^{-1}$ can be assigned to a C═O stretching mode,[28] whereas the large band at 2930 $cm^{-1}$, with a shoulder at about 2825 $cm^{-1}$, can be related to dangling diamond carbon bonds attached to hydrogen atoms that correspond to C−H stretching modes of diamondoids.[29−31] Within the spectral region of 1150−1190 $cm^{-1}$, signals related to trans-polyacetylene are present, whereas other bands between 650 and 1000 $cm^{-1}$ can be assigned to vibrational modes of aromatic hydrocarbon ring structures.[23] The sharp peak at 520 $cm^{-1}$ is referred to the Si substrate.

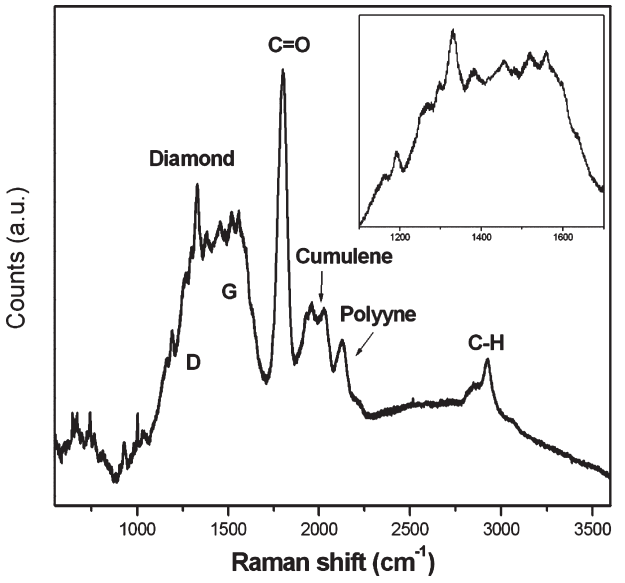


**Figure 4.** SERS spectrum of dried drops of Ag NP colloidal water solution mixed together with PLA species produced by a laser repetition frequency of 1 kHz. In the inset, the 1100−1700 $cm^{-1}$ region is reported to highlight the diamond signal at 1333 $cm^{-1}$. Si(111) substrate.

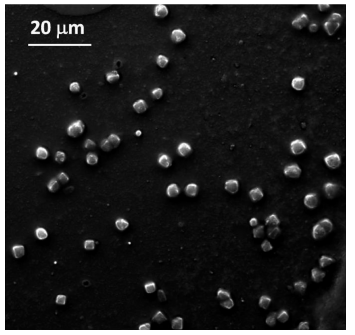


**Figure 5.** SEM image of dried drops of Ag NP colloidal water solution mixed together with PLA species produced by a 10 Hz laser repetition rate. Si(111) substrate.

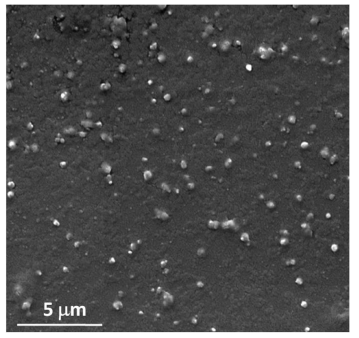


**Figure 6.** SEM image of dried drops of Ag NP colloidal water solution mixed together with PLA species produced by a 1 kHz laser repetition rate. Si(111) substrate.

The different laser repetition rates (10 Hz, 100 Hz, 1 kHz) have a strong effect on the features of the resulting samples. Figures 5 and 6 show SEM images of two different samples, respectively, obtained at 10 Hz and at 1 kHz. Figure 5 shows the


dx.doi.org/10.1021/jp1094239 |J. Phys. Chem. C 2011, 115, 5160–5164

presence of dispersed octahedral-shaped structures with a size ranging from 1 to 5 $\mu$m. The same features are observed in the samples obtained at a repetition rate of 100 Hz. Figure 6 shows mainly the presence of agglomerates of particles having a maximum dimension not exceeding 300 nm.

The experimental data here reported show a quite different growth of DLC and NDs species when a different frequency rate of a femtosecond laser pulsed is used in PLA of graphite in water. In particular, at a 1 kHz laser repetition rate, the growth of NDs occurs as showing the typical SERS signal at 1333 $cm^{-1}$. Furthermore, the band at 2825−2930 $cm^{-1}$ assigned to C−H stretching modes implies the presence of diamond carbon atoms bonded to hydrogen. A band at 1805 $cm^{-1}$ associated with C═O stretching is present in all samples examined, with a relative intensity much more pronounced in samples obtained at a 1 kHz frequency rate. On the other hand, lower laser frequency rates determine the formation of species whose SERS spectra show an O−H stretching mode.

On this basis, two different regimes of condensation and growth of species generated by femtosecond PLA can be obtained simply by varying the laser frequency rate. In particular, when the 1 kHz laser repetition rate is applied, the water cavitation bubble expansion dynamics could lead toward adequate physical−chemical conditions that can drive the process to ND growth.

This hypothesis is confirmed by experimental data available in the literature showing that nanosecond laser ablation of graphite in water produces a shock wave (SW) lasting few hundreds of microseconds.[32] As a consequence, laser repetition rates up to 2 kHz can be applied without generating reflection or absorption of the incoming laser pulse by the plasma-induced SW.[32] Even though the laser pulse used in the present work has a duration of 100 fs, these experimental data can be applied, in first approximation, in order to establish the role played by the variation of the repetition rate of the ultrashort laser pulse here employed. Hence, successive laser shots at a 1 kHz repetition rate may generate PLA of species that expand in favorable thermodynamic conditions self-sustained by the SW induced by them, which can allow the growth of $sp^3$ NDs. Moreover, the layer of water in extreme situations (high pressures and relatively high temperatures) determined by its contact with the SW induced by the expanding plasma may reasonably contain reactive atoms or molecules of dissociated water (e.g., $H_2$, H, O, $O_2$, OH).

The presence of oxygen in chemical vapor deposition (CVD) of diamonds can improve the NDs' quality because the growth of nondiamond $sp^2$ graphitic phases may be inhibited or etched.[33−38] With this regard, it can be hypothesized that, at a 1 kHz laser repetition rate, the surrounding environment of the hybridized $sp^3$ carbons can achieve the NDs' thermodynamic nucleation and growth requirements, together with the presence of local chemical species that do not allow the condensation of the nondiamond phase and are able to favor local oxidation of NDs.[39−41] On the contrary, when the laser repetition rate is decreased to 100−10 Hz, the plasma-induced physical−chemical properties needed for a proper ND growth could not be achieved so that the DLC nondiamond phase can form. The larger dispersion of submicrometer agglomerates obtained at 1 kHz, and not at 10 or 100 Hz, may be interpreted in two ways. The 1 kHz repetition rate laser pulses can generate a large number of nucleation centers that, different than at lower laser rates, grow independently one from another. The 1 kHz repetition rate of the pulses can interact with the formed nanostructures, leading to their fragmentation, thus reducing their dimension and, consequently, increasing the density of NDs dispersed in solution.

## 4. CONCLUSIONS

The repetition rate changes can induce DLC species or ND formation at 10−100 Hz and 1 kHz, respectively, when a 100 fs pulsed laser beam is used for ablating graphite in water. These results suggest that, in these experimental conditions, the laser repetition rate is a key parameter for controlling nucleation and growth of diamond nanoparticles. It has been hypothesized that the shock wave cavitation bubble dynamics, induced by the laser plasma expansion, may achieve the needed physical−chemical features for ND nucleation and growth when a 1 kHz laser repetition rate is used. These conditions might be self-sustained by the short interpulse delay between successive laser pulses. At a 1 kHz laser repetition rate, the physical−chemical features induced by the cavitation bubble expanding in water may be so rapidly regenerated that ND formation can be preserved. When laser repetition rates are diminished of 1 order of magnitude, or more, $sp^2$ graphitic phases may grow preferentially than $sp^3$ ND ones.

The SERS spectra show that, when ND signals are observed, even C═O stretching modes occur. This result would imply that the laser ablation process of graphite in water induced by ultrashort laser pulses may involve oxygen species formation, which can inhibit the nondiamond $sp^2$ graphitic growth or cause oxidation of some carbon sites. The presence of these carbonyl groups, if bonded to the NDs, would provide new perspectives for adding functional groups to them and extend the use of PLA in liquid for applications in other relevant fields, such as nanodrug delivery systems.[42,43]

On the basis of the results here presented, future work is planned for evaluating the role played by different confining liquids, for surveying the changes occurring when the produced species undergo thermal treatments, and for assessing the features of the laser-induced plasma dynamics and its relative cavitation bubble and SW properties generated during the ultrashort laser ablation of graphite in liquids.

## AUTHOR INFORMATION

### Corresponding Author

*Telephone: +39 0971 206249. Fax: +39 0971 206250. E-mail: angela.debonis@unibas.it.

## REFERENCES

(1) Ogale, S. B.; Malshe, A. P.; Kanetkar, S. M.; Kshirsagar, S. T. *Solid State Commun.* **1992**, *84*, 371–373.

(2) Yang, L.; May, P. W.; Yin, L.; Smith, J. A.; Rosser, K. N. *Diamond Relat. Mater.* **2007**, *16*, 725–729.

(3) Wang, J. B.; Zhang, C. Y.; Zhong, X. L.; Yang, G. W. *Chem. Phys. Lett.* **2002**, *361*, 86–90.

(4) Pearce, S. R. J.; Henley, S. J.; Claeyssens, F.; May, P. W.; Hallam, K. R.; Smith, J. A.; Rosser, K. N. *Diamond Relat. Mater.* **2004**, *13*, 661–665.

(5) Amans, D.; Chenus, A. C.; Ledoux, G.; Dujardin, C.; Reynaud, C.; Sublemontier, O.; Masenelli-Varlot, K.; Guillois, O. *Diamond Relat. Mater.* **2009**, *18*, 177–180.

(6) Tian, F.; Sun, J.; Hu, S. L.; Du, X. W. *J. Appl. Phys.* **2008**, *104*, 096102.

(7) Sun, J.; Hu, S. L.; Du, X. W.; Lei, Y. W.; Jiang, L. *Appl. Phys. Lett.* **2006**, *89*, 183115.

(8) Wang, C. X.; Liu, P.; Cui, H.; Yang, G. W. *Appl. Phys. Lett.* **2005**, *87*, 201913.
(9) Hu, S.; Sun, J.; Du, X. W.; Tian, F.; Jiang, L. *Diamond Relat. Mater.* **2008**, *17*, 142–146.
(10) Bai, P.; Hu, S.; Zhang, T.; Sun, J.; Cao, S. *Mater. Res. Bull.* **2010**, *45*, 826–829.
(11) Wang, C. X.; Yang, Y. H.; Liu, Q. X.; Yang, G. W. *Appl. Phys. Lett.* **2004**, *84*, 1471–1473.
(12) Yang, G. W.; Wang, J. B.; Liu, Q. X. *J. Phys.: Condens. Matter* **1998**, *10*, 7923–7927.
(13) Wang, J. B.; Yang, G. W. *J. Phys.: Condens. Matter* **1999**, *11*, 7089–7094.
(14) Liu, P.; Wang, C.; Chen, J.; Xu, N.; Yang, G.; Ke, N.; Xu, J. *J. Phys. Chem. C* **2009**, *113*, 12154–12161.
(15) Yang, G. W. *Prog. Mater. Sci.* **2007**, *52*, 648–698.
(16) Tan, D.; Lin, G.; Liu, Y.; Teng, Y.; Zhuang, Y.; Zhu, B.; Zhao, Q.; Qiu, J. *J. Nanopart. Res.* **2010**, DOI: 10.1007/s11051-010-0110-4.
(17) Mafune, F.; Kohno, J. K.; Takeda, Y.; Kondow, T. *J. Phys. Chem. B* **2000**, *104*, 9111–9117.
(18) Zhao, Y.; Jang, Y.; Fang, Y. *Spectrochim. Acta, Part A* **2006**, *65*, 1003–1006.
(19) Jacak, W.; Krasnyj, J.; Gonczarek, R.; Chepok, A.; Jacak, L.; Hu, D. Z.; Schaadt, D. *J. Appl. Phys.* **2010**, *107*, 124317.
(20) Ferrari, A. C.; Robertson, J. *Phys. Rev. B* **2000**, *61*, 14095–14107.
(21) Ferrari, A. C.; Robertson, J. *Phys. Rev. B* **2001**, *63*, 121405.
(22) Tabata, H.; Fujii, M.; Hayashi, S. *Chem. Phys. Lett.* **2006**, *420*, 166–170.
(23) Hu, A.; Lu, Q. B.; Duley, W. W.; Rybachuk, M. *J. Chem. Phys.* **2007**, *126*, 154705.
(24) Tabata, H.; Fujii, M.; Hayashi, S.; Doi, T.; Wakabayashi, T. *Carbon* **2006**, *44*, 3168–3176.
(25) Lucotti, A.; Casari, C. S.; Tommasini, M.; Li Bassi, A.; Fazzi, D.; Russo, V.; Del Zoppo, M.; Castiglioni, C.; Cataldo, F.; Bottani, C. E.; Zerbi, G. *Chem. Phys. Lett.* **2009**, *478*, 45–50.
(26) Casari, C. S.; Li Bassi, A.; Ravagnan, L.; Siviero, F.; Lenardi, C.; Piseri, P.; Bongiorno, G.; Bottani, C. E.; Milani, P. *Phys. Rev. B* **2004**, *69*, 075422.
(27) Hu, A.; Rybachuck, M.; Lu, Q. B.; Duley, W. W. *Appl. Phys. Lett.* **2007**, *91*, 131906.
(28) Gibson, N.; Shenderova, O.; Luo, T. J. M.; Moseenkov, S.; Bondar, V.; Puzyr, A.; Purtov, K.; Fitzgerald, Z.; Brenner, D. W. *Diamond Relat. Mater.* **2009**, *18*, 620–626.
(29) Filik, J.; Harvey, J. N.; Allan, N. L.; May, P. W.; Dahl, J. E. P.; Liu, S.; Carlson, R. M. K. *Spectrochim. Acta, Part A* **2006**, *64*, 681–692.
(30) Dahl, J. E.; Liu, S. G.; Carlson, R. M. K. *Science* **2003**, *299*, 96–99.
(31) Dahl, J. E. P.; Moldowan, J. M.; Peakman, T. M.; Clardy, J. C.; Lobkovsky, E.; Olmstead, M. M.; May, P. W.; Davis, T. J.; Steeds, J. W.; Peters, K. E.; Pepper, A.; Ekuan, A.; Carlson, R. M. K. *Angew. Chem., Int. Ed.* **2003**, *42*, 2040–2044.
(32) Sajti, C. L.; Sattari, R.; Chichkov, B. N.; Barcikowski, S. *J. Phys. Chem. C* **2010**, *114*, 2421–2427.
(33) Oake, D. B.; Butler, J. E.; Snail, K. A.; Carrington, W. A.; Hanssen, L. M. *J. Appl. Phys.* **1991**, *69*, 2602–2610.
(34) Ando, Y.; Tachibana, T.; Kobashi, K. *Diamond Relat. Mater.* **2001**, *10*, 312–315.
(35) Yarbrough, W. A.; Messier, R. *Science* **1990**, *247*, 688–696.
(36) Liou, Y.; Inspektor, A.; Weimer, R.; Knight, D.; Messier, R. *J. Mater. Res.* **1990**, *5*, 2305–2312.
(37) Tang, C. J.; Pereira, S. M. S.; Fernandes, A. J. S.; Neves, A. J.; Grácio, J.; Bdikin, I. K.; Soares, M. R.; Fu, L. S.; Gu, L. P.; Kholkin, A. L.; Carmo, M. C. *J. Cryst. Growth* **2009**, *311*, 2258–2264.
(38) Das, D.; Singh, R. N.; Barney, I. T.; Jackson, A. G.; Mukhopadhyay, S. M. *J. Vac. Sci. Technol., A* **2008**, *26*, 1487–1496.
(39) Chakrapani, V.; Angus, J. C.; Anderson, A. B.; Wolter, S. D.; Stoner, B. R.; Sumanasekera, G. U. *Science* **2007**, *318*, 1424–1430.
(40) Maier, F.; Riedel, R.; Mantel, B.; Ristein, J.; Ley, L. *Phys. Rev. Lett.* **1990**, *85*, 3472–3475.
(41) Fink, C. K.; Jenkins, S. J. *J. Phys.: Condens. Matter* **2009**, *21*, 264010.
(42) Krueger, A. *Adv. Mater.* **2008**, *20*, 2445–2449.
(43) Schrand, A. M.; Ciftan Hens, S. A.; Shenderova, O. A. *Crit. Rev. Solid State Mater. Sci.* **2009**, *34*, 18–74.